Studying meson-nucleus interactions - the long way to indications for the existence of mesic states

Volker Metag[1,*]
for the CBELSA/TAPS, η-PRiME, and Super-FRS-Experiment collaborations

[1]II. Physikalisches Institut, Universität Gießen, Germany

Abstract. So far, no system consisting of a nucleus and a neutral meson that is bound purely by the strong interaction has been observed. This article describes the long way from studying the η'-nucleus interaction to first indications of the existence of bound states of the η'-meson and a nucleus. Photo-production of η'- mesons off nuclei has revealed a strong attraction together with weak absorption, making the η' meson a promising candidate for the search for mesic states, since well-separated narrow bound states can only be observed if their widths are much smaller than their spacing. Experiments aimed at directly populating η' -mesic states used missing mass spectrometry in the ^{12}C(p,d) reaction. By tagging the decay of η' -mesic states via the channel η'Np $\rightarrow$Np, structures in the bound state region have been observed that are consistent with calculations predicting the existence of η'-mesic states with a potential depth of $V_0 = -(61 \pm 1(\text{stat}) \pm 5(\text{syst}))$ MeV and an imaginary potential $|W_0| \leq 10$ MeV. This implies a drop in the mass of the η' meson by ≈ 61 MeV at normal nuclear matter density relative to its mass in vacuum. The statistical significance of the structures of presently 3.5 σ can hopefully be improved in a further optimised experiment which is in preparation.

1 Introduction

In physics, we are familiar with different interactions and correspondingly different types of bound systems. Earth and Moon are bound by gravitation; nuclei and electrons are bound to atoms by the electromagnetic interaction. Pionic or kaonic atoms, in which one of the electrons is replaced by a negatively charged meson, are also mainly bound by the electromagnetic interaction; the strong interaction introduces only minor, yet significant, modifications to the energy and width of the bound atomic states. A nucleus and a neutral meson, such as ω, η, or η', can only be bound by the strong interaction. Such a system has not yet been observed. The first step in finding such a system is to establish whether the meson-nucleus interaction is attractive rather than repulsive. Thus, the parameters of the meson-nucleus optical potential must be determined. The Cracow group, led by P. Moskal and M. Skurzok [1], has conducted thorough studies of the η-nucleus system at COSY and has managed to restrict the potential parameters for possible η-nucleus bound states in light nuclei. Here, the focus is on the η'-meson.

*e-mail: volker.metag@exp2.physik.uni-giessen.de

The η'-meson is the heaviest of the pseudoscalar mesons, with 957.8 MeV - even heavier than the nucleon. How do these mesons get their mass? Theorists addressed this question in the 1990s [2, 3], but it remains a fundamental issue in hadron physics nowadays [4]. Dynamically breaking chiral symmetry by a non-zero chiral condensate yields a nonet of massless pseudoscalar mesons. Breaking axial U(1) symmetry via gluonic effects in the singlet channel results in a mass splitting into a massive singlet η_0 and an octet of still massless pseudoscalar mesons. Explicit breaking of chiral symmetry by introducing non-zero quark masses yields the experimentally observed meson masses listed in the PDG [5]. Given the significant impact of symmetry breaking on meson masses, one would also anticipate mass changes in case of a partial restoration of this symmetry, as predicted by theory and evidenced by experimental findings from pionic atoms [6]. Therefore, the masses of mesons are expected to change when they are embedded in a nuclear medium. In particular, partial restoration of chiral symmetry in a nuclear environment would suppress the $U_A(1)$ anomaly effect on the η'-mass, leading to a reduction of its mass in the medium compared to its mass in vacuum. While these are only qualitative arguments, various model calculations have been performed by different theory groups to make quantitative predictions for changes of the η'-meson mass in nuclei. Within the Nambu-Jona-Lasinio model Bernard and Meissner [7] predicted only a weak dependence of the η'- mass on nuclear density. In contrast, Nagahiro et al.[8], using the same model, predicted a mass drop of the η'- by about 150 MeV at normal nuclear matter density. In a linear sigma model Sakai and Jido [9] found a lowering of the η'-mass by 80 MeV and in the quark-meson-coupling model a mass drop by 40 MeV [10] or 60 MeV [11] at normal nuclear matter has been predicted. Although all theoretical calculations agree that the η' mass should be lowered in a nuclear medium, there is a wide range of predictions, calling for the experiments, described in the following sections.

2 The η'-nucleus potential from photo-nuclear reactions

The real part V(r) of the complex meson-nucleus potential is related to the mass change Δm and the imaginary part W(r) describes the absorption of the meson by interactions with the nucleons [12].

$$U(r) = V(r) + iW(r) \tag{1}$$

$$V(r) = \Delta m(\rho_0) \cdot \frac{\rho(r)}{\rho_0}; \qquad W(r) = -\frac{\Gamma_0}{2} \cdot \frac{\rho(r)}{\rho_0} = -\frac{1}{2}\hbar c \cdot \rho(r) \cdot \sigma_{inel} \cdot \beta \tag{2}$$

Hereby $\rho(r)$ is the nuclear density profile, ρ_0 and Γ_0 are the nuclear density and the in-medium meson width at the center of the nucleus, respectively, and β is the velocity of the meson relative to the speed of light. The real part can be determined experimentally by measuring excitation functions and momentum distributions as well as through spectroscopy of meson-nucleus bound states. The imaginary part of the potential can be determined from the so-called transparency ratio [13] where one compares the meson production cross section off a nucleus per nucleon with the production cross section off a free nucleon.

$$T_A = \frac{\sigma_{\gamma A \to mX}}{A \cdot \sigma_{\gamma N \to mX}} \tag{3}$$

If there were no absorption, this ratio would be one, but any deviation from one indicates the size of the inelastic cross section $\sigma_{inel.}$, from which the imaginary part of the meson-nucleus potential can be determined using Eq. 2.

The following qualitative arguments demonstrate that excitation functions and meson momentum distributions are sensitive to a drop in the meson mass in the medium. In the case of

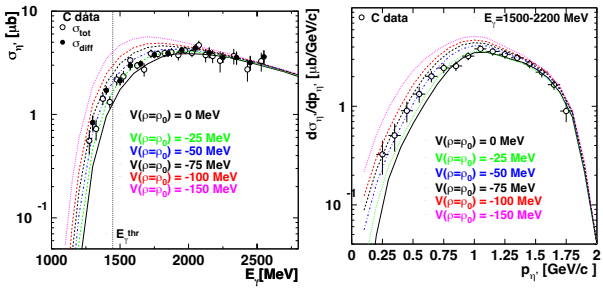

Figure 1. Measured excitation function and momentum differential cross section for η' meson photo-production off ^{12}C [16] in comparison to collision model calculations for different potential depths [15]. The solid black curve corresponds to the case $V_0 = 0$, i.e. no further interaction of the η' meson with the nucleus.

an attractive meson-nucleus interaction, the effective meson mass decreases and the production threshold is lowered. Consequently, the phase space increases, yielding a larger cross section near the threshold compared to the case $V_0 = 0$ without mass modification. In case of a repulsive interaction the in-medium mass and the production threshold increase, reducing the phase space and leading to a smaller cross section. The cross sections for all scenarios converge at energies much higher than the threshold. Similar qualitative arguments apply to the momentum differential cross section. In the case of an attractive meson-nucleus interaction the meson is slowed down on its way out, resulting in a shift of the momentum distribution towards lower momenta. For a repulsive meson-nucleus interaction, the meson receives an additional boost, leading to a shift of the momentum distribution towards higher momenta. Again, for energies much larger than the production threshold, all distributions will merge. Thus, for an attractive interaction, a cross section enhancement near threshold and a shift of the momentum distribution towards lower values is expected. For a quantitative analysis, the data have to be compared with transport calculations, e.g. GiBUU [14] or collision model calculations [15], which unfortunately makes these results model dependent to some extent.

But how does one obtain the imaginary part? The produced meson can either leave the nucleus without interacting further, or be removed by an inelastic reaction on another nucleon. The relative strength of these processes determines the transparency ratio (Eq. 3). Having determined the inelastic cross section by comparing the experimental transparency ratio with model calculations, the imaginary potential can be deduced (Eq. 2).

The η'-excitation functions, momentum distributions and transparency ratios have been measured in photo-production reactions at the CBELSA/TAPS detector located at the electron accelerator ELSA in Bonn, using a tagged photon beam up to energies of 3.2 GeV. This detector has an almost 4π acceptance which is required to reconstruct the η' meson via the $\eta' \to \pi^0\pi^0\eta \to 6\gamma$ decay mode. An invariant mass resolution of 1% has been achieved for all nuclear targets [16].

The η'-excitation function and momentum distribution measured on a C target are shown in Fig. 1 [17] in comparison to model calculations [15]. The black solid curves in both plots correspond to the V_0=0 case, i.e., no further interaction of the produced η' meson with the nucleus as in η' photo-production off a free proton. The data show a cross section enhancement near threshold and a shift of the η' momentum distribution towards lower momenta - a clear signature of an attractive η'-nucleus interaction. To determine the potential parameters quantitatively, the data are compared to model calculations for different potential depths of the real part of the η' -nucleus potential [15]. This comparison disfavours very strong mass shifts; best agreement between data and calculations is found for potential depths of the order of 30-40 MeV [17]. Similar results are obtained for the Nb target [18]; again a cross section enhancement near threshold and a shift towards lower momenta are observed. Potential depths of the order of 40 MeV are deduced. Taking the weighted average of all cross section and momentum distribution measurements gives a real part of the η'-nucleus potential of -(40±7(stat)±15(syst)) MeV.

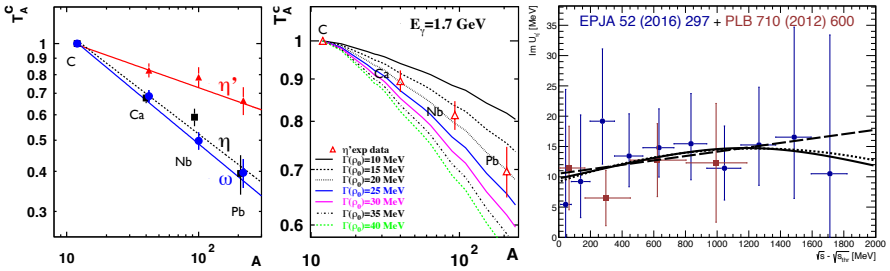

Figure 2. (Left) Transparency ratio normalised to C for photo-production of η', η and ω mesons as a function of the nuclear mass number [19]. (Middle) Comparison of measured transparency ratios with model calculations for different in-medium η' widths [16]. (Right) Dependence of the deduced imaginary part of the η'-Nb potential as function of the energy above the production threshold [21].

To determine the imaginary part, the measured transparency ratios for η', η and ω mesons are shown in Fig. 2[19]. The transparency ratios decrease as a function of mass number, however, much weaker absorption is observed for the η' meson than for η and ω mesons. A comparison with model calculations indicates values of the absorptive width of the order of 15-25 MeV for the η' meson-[17]. As it is important to know the imaginary part of the potential near threshold because this determines the widths of possible bound states, the momentum dependence of the transparency ratio has also been measured [20, 21]. The imaginary part of the potential deduced from these measurements is plotted as a function of the energy above threshold in Fig. 2 (Right). Extrapolating to the production threshold yields an imaginary potential of 10±4(stat)±2(syst) MeV [21], implying that the imaginary part is only about a quarter of the real part. This makes the η' meson a promising candidate for searching for mesic states [22], since bound states can only be identified experimentally if their width is small compared to their energy spacing.

3 The direct population of η'- mesic states

These photo-nuclear results supported the proposal by K. Itahashi et al. [23] to directly populate η' mesic states in the ^{12}C(p,d)η'X reaction, as illustrated in Fig. 3 (Left). A 2.5 GeV proton beam impinging on a ^{12}C target produces an η' meson. In this neutron pick up reaction the forward-going deuteron takes over most of the momentum of the incident beam, leaving little energy for the η' meson, which can then be bound to the carbon nucleus if there is an attractive interaction. This is a two-body final state, so measuring the deuteron momentum is sufficient to determine the excitation energy of η'-mesic carbon. Allowing for a narrow range in momentum, one can select an excitation energy spectrum near the η'-production threshold. Theoretical predictions for such an excitation energy spectrum showed several rather narrow states in the bound state region [4]. However, the corresponding experimental spectrum taken at the GSI fragment separator showed no sign of narrow structures [24]. A comparison of the theoretical and experimental cross sections revealed that the experimental spectrum was dominated by background. Still, this negative result enabled a limit to be set on the η' ^{11}C - nucleus potential of less than 100 MeV [25].

The sensitivity of the experiment can be improved by tagging the decay of the η' mesic states [25, 26]. What are the obvious decay modes? The η' meson bound to ^{11}C can interact with a nucleon of ^{11}C to produce a pion or an η meson. The decay mode η'p$\rightarrow$ η p was investigated by the group at Spring 8 [27] but they were only able to constrain the potential parameters of possible η' mesic states. In the case of two-body absorption, the decay channel would be η' Np $\rightarrow$ Np, for which theoretical calculations predict a branching ratio of about 50% [28]. Due to the high η' mass, both nucleons acquire a very high momentum of about 1 GeV/c each, much higher than the proton momenta from background processes or meson

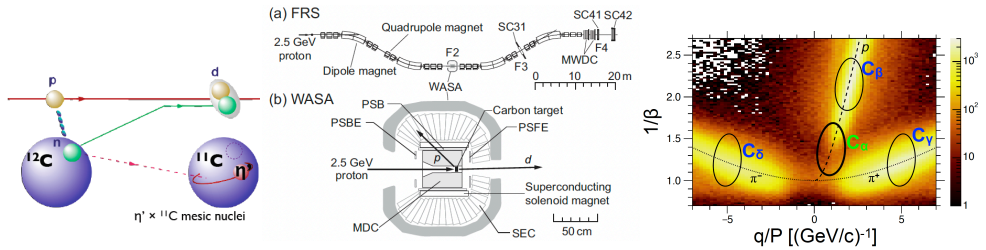

Figure 3. (Left) Illustration of populating an η' mesic state in the ^{12}C(p,d)η'X reaction. (Middle) Experimental setup at GSI (Darmstadt, Germany) with fragment separator FRS and the WASA detector surrounding the target [30]. (Right) Particle identification with the WASA detector [30].

decays. While most of the charged particles produced in the reaction will move forward due to the boost from the incoming proton beam, protons from the two-body absorption process will be distributed almost isotropically, since the η'-mesic ^{11}C are nearly at rest in the laboratory. Thus, one has to look for ≈ 1 GeV/c protons at backward angles [29].

The essential improvement compared to the first experiment at GSI is the WASA detector at the target position (Fig. 3 (Middle)) for tracking the decay particles of the η'-mesic states in a magnetic field [30], in coincidence with the forward-going deuterons. As before, the 2nd half of the FRS is used to measure the momentum of the deuterons to determine the excitation energy of ^{11}C. With a momentum acceptance of the FRS of ±3% an excitation energy range of η'mesic carbon of ± 60 MeV around the η' production threshold can be covered. During a 3-day data taking period 10^7 ^{12}C(p,d) events were recorded [30]. For identifying the particles

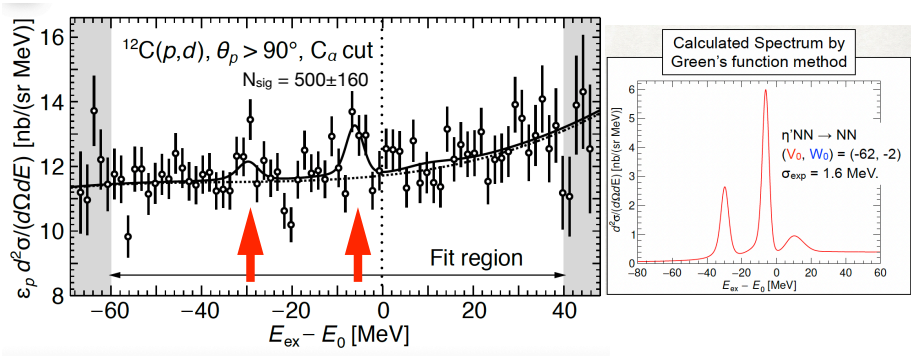

Figure 4. Excitation energy spectrum of the ^{12}C(p,d) reaction near the η' production threshold E_0 measured in coincidence with high-momentum, backward-going protons for the cut condition C_α. The solid curve represents a fit with the theoretically expected pattern for (V_0,W_0) = (-62,-2) MeV. The dotted curve represents the pedestal fit [30].

registered in WASA, the time-of-flight information, the energy loss and the momentum of the charged particles are used, as described by R. Sekiya in his contribution to this conference [30]. Plotting $1/\beta$ versus charge over momentum q/p in Fig. 3 (Right) one can easily identify a proton, π^+ and π^- branch. C_α is the cut region where protons from the η' Np → Np, decay of a possible η' mesic state are expected. The other cuts are off-signal cuts for studying the background. Corresponding excitation energy spectra are all quite flat and do not exhibit any significant structures.

The excitation energy spectrum for the cut condition C_α is shown in (Fig. 4 (Left)), exhibiting structures in the bound state region at ≈ - 6 MeV and ≈ -30 MeV as well as an increase in yield above the η' production threshold, indicated by the dotted line. This yield can probably be attributed to η' mesons produced above threshold, trying to leave the ^{11}C

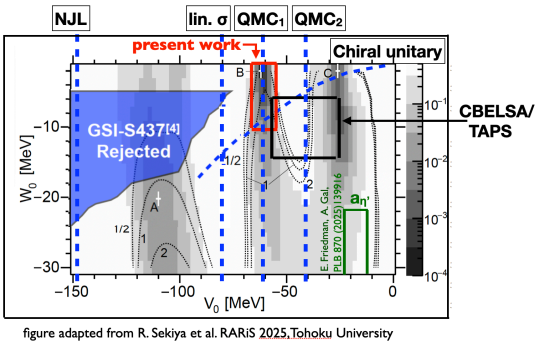

Figure 5. Experimentally determined potential parameters of η'-mesic ^{11}C in comparison to theoretical predictions [31].The green box marks parameters deduced by A. Gal [32, 33] from measured η'-p scattering lengths [34, 35]. The blue shaded area shows the parameter range excluded in [24, 25].

nucleus, but which are stopped on their way out by two-body absorption in the η' Np $\rightarrow$ Np channel. To enable comparison with theoretical predictions, 1140 spectra were calculated with the Green's function method for different real and imaginary potentials ranging in V_0 from -150 to 0 MeV and in W_0 from -2 to -30 MeV, each in steps of 2 MeV. Similar to the experimental spectrum, the spectrum calculated for V_0= -62 MeV and W_0= -2 MeV (Fig. 4 (Right) shows a pattern of 2 states separated by approximately 24 MeV, given by the $\hbar\omega$ of the ^{12}C nuclear potential. Fitting the calculated pattern (solid curve) to the experimental spectrum gives χ^2/ndf = 65.4/62 compared to χ^2/ndf = 77.4/63 for the null hypothesis (dotted curve). The difference in χ^2 corresponds to a local p_0 value of $2.6{\cdot}10^{-4}$ and a significance of 3.5 σ. Thus, the probability that the observed structures are due to fluctuations is $2.6 \cdot 10^{-4}$. Considering the look-elsewhere-effect, the significance reduces to 2.5 σ. Other parameter pairs have been investigated by Sekiya [30], but the optimal potential parameters are found to be V_0= - (61 $\pm$ 1(stat) $\pm$ 5(syst)) MeV and $|W_0| \leq 10$ MeV.

Fig. 5 shows a comparison of theoretical predictions and experimental results for the imaginary versus real potential of the η' - nucleus interaction [31]. While the WASA@FRS and photo-nuclear results show an overlap within errors, deviating values are derived by Friedman and Gal [32, 33] from measured η'-p scattering lengths [34, 35]. This difference may indicate a strong energy dependence of the η'-p scattering amplitude near the η' production threshold, as found in the η-p system [36], and requires further study.

4 Summary

Studying photo-production of η' mesons off nuclei, the interaction between an η' meson and a nucleus has been found to be attractive with only weak absorption which makes the η'-meson a good candidate for the search for meson-nucleus bound states. This strengthened the case for directly looking for η' bound states. While the first experiment was not sensitive enough, the second experiment, which involved tagging the decay of the η'-mesic states revealed narrow structures in the bound state region, consistent with calculations that predict the existence of η'-mesic states. First indications for a meson-nucleus system bound only by the strong interaction may have been found. The mass of the η' meson in a nuclear medium at normal nuclear matter density is found to be $\approx$ 60 MeV lower than in vacuum. As the statistics obtained in a 3-day experiment is limited, a longer beam time and a further optimised experiment with a new magnet operating at a higher field are planned to improve the experimental significance.

I would like to thank all members of the CBELSA/TAPS, η-PRiMEPrime, and Super-FRS Experiment collaborations. Without their valuable contributions it would not have been possible to obtain the results presented here. In particular, I would like to thank my long-time collaborator M. Nanova and the Japanese colleagues R. Sekiya, Y. Tanaka, K. Itahashi, S. Hirenzaki, N. Ikeno, and J. Yamagata-Sekihara who played the leading role in the direct search for η' mesic states.

References

[1] M. Skurzok, Status of the Search for η-Mesic Nuclei with Particular Focus on η-Helium Bound states. Few-Body Syst. **62**, 5 (2021). https://doi.org/10.1007/s00601-020-01585-x

[2] V. Bernard et al., Strangeness mixing and quenching in the Nambu-Jona-Lasinio model. Nucl. Phys. B **308**, 753 (1988)

[3] S. Klimt et al., Generalized SU(3) Nambu-Jona-Lasinio Model. Nucl. Phys. A **516**, 429 (1990)

[4] H. Nagahiro et al., Formation of η'(958)-mesic nuclei by the (p,d) reaction. Phys. Rev. C **87**, 045201 (2013). DOI: 10.1103/PhysRevC.87.045201

[5] Particle Data Group, S. Navas et al., Review of Particle Physics. Phys. Rev. D **110**, 030001 (2024). DOI: https://doi.org/10.1103

[6] T. Nishi et al., Chiral symmetry restoration at high matter density observed in pionic atoms. Nature Phys. **19**, 788 (2023). https://doi.org/10.1038/s41567-023-02001-x

[7] V. Bernard and U.-G. Meissner, Meson properties at finite density from $SU(3)_f$ quark dynamics. Phys. Rev. D **38**, 1551(1988)

[8] H. Nagahiro et al., η- and η'-mesic nuclei and $U_A(1)$ anomaly at finite density. Phys. Rev. C **74**, 045203 (2006). DOI: 10.1103/PhysRevC.74.045203

[9] S. Sakai and D. Jido, In-medium η' mass and η'N interaction based on chiral effective theory. Phys. Rev. C **88**, 064906 (2013). DOI: 10.1103/PhysRevC.88.064906

[10] S. Bass and A. Thomas, η bound states in nuclei: a probe of flavour-singlet dynamics. Phys. Lett. B **634**, 368 (2006). doi:10.1016/j.physletb.2006.01.071

[11] J.J. Cobos-Martinez and K. Tsushima, η and η' mesons in nuclear matter and nuclei. Phys. Rev. C **109**, 025202 (2024). DOI: 10.1103/PhysRevC.109.025202

[12] H. Nagahiro and S. Hirenzaki, Formation of η'(958)-Mesic Nuclei and Axial $U_A(1)$ Anomaly at Finite Density. Phys. Rev. Lett. **94**, 232503 (2005). DOI: 10.1103/PhysRevLett.94.232503

[13] D. Cabrera et al., Mass dependence of inclusive nuclear Φ photoproduction. Nucl Phys. A **733**, 130 (2004). doi:10.1016/j.nuclphysa.2003.12.012

[14] O. Buss et al., Transport-theoretical description of nuclear reactions. Phys. Rep. **512**, 1 (2012), http://gibuu.hepforge.org. doi:10.1016/j.physrep.2011.12.001

[15] E. Paryev, Photoproduction of η' mesons from nuclei and their properties in the nuclear medium. J. Phys. G **40**, 025201 (2013). doi:10.1088/0954-3899/40/2/025201

[16] M. Nanova et al., Transparency ratio in $\gamma A \to \eta' A'$ and the in-medium η' width. Phys. Lett. B **710**, 600 (2012). http://dx.doi.org/10.1016/j.physletb.2012.03.039

[17] M. Nanova et al., Determination of the η'-nucleus optical potential. Phys. Lett. B **727**, 417 (2013). http://dx.doi.org/10.1016/j.physletb.2013.10.062

[18] M. Nanova et al., Determination of the real part of the η' -Nb optical potential. Phys. Rev. C **94**, 025201 (2016). http://dx.doi.org/10.1016/j.physletb.2013.10.062

[19] V. Metag et al., Determination of the meson-nucleus potential - on the way to mesic states. Hyp. Int. **234**, 25 (2015). DOI: 10.1007/s10751-015-1135-y

[20] S. Friedrich et al., Momentum dependence of the imaginary part of the ω- and η'-nucleus potential. Eur. Phys. J. A **52**, 297 (2016). DOI 10.1140/epja/i2016-16297-4

[21] S. Friedrich et al., Addendum to: Momentum dependence of the imaginary part of the ω- and η'-nucleus potential. Eur. Phys. J. A **62**, 177 (2026). https://doi.org/10.1140/epja/s10050-026-01908-2

[22] V. Metag, M. Nanova, and E. Paryev, Meson-Nucleus potentials and the search for meson-nucleus bound states. Prog. Part. Nucl. Phys. **97**, 199 (2017).

http://dx.doi.org/10.1016/j.ppnp.2017.08.002

[23] K. Itahashi et al., Feasibility Study of Observing η' Mesic Nuclei with (p,d) Reaction. Prog. Theo. Phys. **128**, 601 (2012)

[24] Y. Tanaka et al., Measurement of Excitation Spectra in the $^{12}C(p,d)$ Reaction near the η' Emission Threshold. Phys. Rev. Lett. **117** 202501 (2016). DOI: 10.1103/PhysRevLett.117.202501

[25] Y. Tanaka et al., Missing-mass spectroscopy of the $^{12}C(p,d)$ reaction near the η' production threshold. Phys. Rev. C **97** 015202 (2018). DOI: 10.1103/PhysRevC.97.015202

[26] H. Fujioka et al., Spectroscopy of η'-nucleus bound states at GSI and FAIR - very preliminary results and future prospects. Hyp. Int. **234**, 33 (2015). DOI 10.1007/s10751-015-1145-9

[27] N. Tomida et al., Search for η' Bound Nuclei in the $^{12}C(\gamma, p)$ Reaction with Simultaneous Detection of Decay Products. Phys. Rev. Lett. **124** 202501 (2020). DOI: 10.1103/PhysRevLett.124.202501

[28] H. Nagahiro, S. Hirenzaki, E. Oset, and A. Ramos, η'-nucleus optical potential and η' bound states. Phys. Lett. B **709** 87 (2012). doi:10.1016/j.physletb.2012.01.061

[29] N. Ikeno et al., Feasibility of the Observation of η' Mesic Nuclei in the Semi-Exclusive $^{12}C(p,dp)$ Reaction. PTEP **2026** 073D05 (2026). DOI: 10.1093/ptep/ptag114

[30] R. Sekiya et al., ExcitationSpectra of the $^{12}C(p,d)$ Reaction near the η'-Meson Emission Threshold Measured in Coincidence with High-Momentum Protons. Phys. Rev. Lett. **136** 142501 (2026). DOI: 10.1103/6vsl-ng7x and contribution to this conference

[31] R. Sekiya et al., RARiS 2025,Tohoku University

[32] E. Friedman and A. Gal, Revisiting $\eta'(958)$ nuclear states. Phys. Lett. B **870** 139916 (2025). https://doi.org/10.1016/j.physletb.2025.139916

[33] A. Gal, contribution to this conference

[34] E. Czerwinski et al., Determination of the η'- Proton Scattering Length in Free Space. Phys. Rev. Lett. **113** 062004 (20214). DOI: 10.1103/PhysRevLett.113.062004

[35] A.V. Anisovich et al., Proton-η' interactions at threshold. Phys. Lett. B **785** 626 (2018). https://doi.org/10.1016/j.physletb.2018.06.034

[36] A. Cieply et al., In-medium ηN interactions and η nuclear bound states. Nucl. Phys. A **925** 126 (2014). http://dx.doi.org/10.1016/j.nuclphysa.2014.02.007